Long-Time Evolution of Semiclassical States in Anharmonic Potentials

P. Kasperkovitz and M. Peev
Institut für Theoretische Physik, Technische Universität Wien, Wiedner Hauptstrasse 8-10, A-1040 Wien, Austria
(Received 24 March 1995)

We study numerically the one-dimensional quantum evolution of a coherent state when the particle is bound by a nonlinear force. Snapshots of the Husimi function show that there exist times where the initial Gaussian distribution in phase space splits into chains of $2, 3, \ldots$ distributions of similar form. During their finite lifetime the members of such a string are equally distributed along the classical orbit which passes through the center of the initial distribution, and they move along this curve with the corresponding velocity. This effect, which is generic for integrable bounded motion, is explained in terms of the quantum analogs of action and angle variables.

PACS numbers: 03.65.Ge, 03.20.+i, 03.65.Sq

Although quantum mechanics (QM) is usually formulated in terms of state vectors and operators, it was discovered more than half a century ago [1] that it is possible to cast this theory in a form which closely resembles classical statistical mechanics (CM). Nowadays it is known that there exist infinitely many of such quasiclassical theories which are equivalent to standard QM. The most famous phase-space equivalents of the density operator are the Wigner function [1,2] and the Husimi function [3]; more recently, the latter is favored by many authors because it is a strictly positive function which makes the comparison of CM and QM more intuitive [4]. No matter which formalism is used, both the basic equations and the examples which can be treated by analytical or numerical methods clearly show two fundamental differences between QM and CM: (i) Because of the uncertainty principle, the set of phase-space representatives of quantum states is more restricted than the set of classical states [5]. (ii) If one starts with an initial distribution, which can be interpreted both as classical and as a quantum state, its evolution in time differs essentially in the two theories, provided the period of observation is sufficiently long.

In this contribution we discuss the evolution of coherent states in anharmonic potentials:

$$t = 0: \quad \psi_{p_0,x_0}(x) = \langle x \mid p_0, x_0 \rangle = \pi^{-1/4} \exp\left\{ i \frac{p_0}{\hbar} - \frac{\hbar (x - x_0)^2}{2} \right\}, \tag{1}$$

$$H(p,x) = \tfrac{1}{2} p^2 + c\,|x|^\nu, \quad c > 0,\ 2 < \nu \leq \infty. \tag{2}$$

$\nu = \infty$ is the infinitely deep square well for which all results may be obtained in closed form [6]. It suffices to consider only one-dimensional motion, because the following considerations are easily generalized to integrable bounded systems with more degrees of freedom. The effects we are going to discuss can be seen in the evolution of various time-dependent quantities: wave function, Wigner or Husimi function, expectation values, correlation functions, etc. We prefer to display snapshots of the Husimi function for the following two reasons: (i) It turned out that the observed patterns are closely related to the fact that the classical motion takes place on invariant tori (closed curves in the present case); hence a phase-space formulation of quantum mechanics is most suited for explanation. (ii) The rapid oscillations in classically forbidden regions which are usually observed for Wigner functions are absent in the corresponding Husimi functions so that essential features common to both functions are more easily perceived in the latter.

Figure 1 shows the Husimi function

$$F_{p_0,x_0}(p,x,t) = \left| \langle p,x \mid \hat{U}_t \mid p_0,x_0 \rangle \right|^2 \tag{3}$$

at $t = 0$: a Gaussian centered at $p_0 > 0$, $x_0 = 0$ whose width is proportional to $\sqrt{\hbar}$. The closed curves are contour lines of the Hamiltonian (2), or the classical

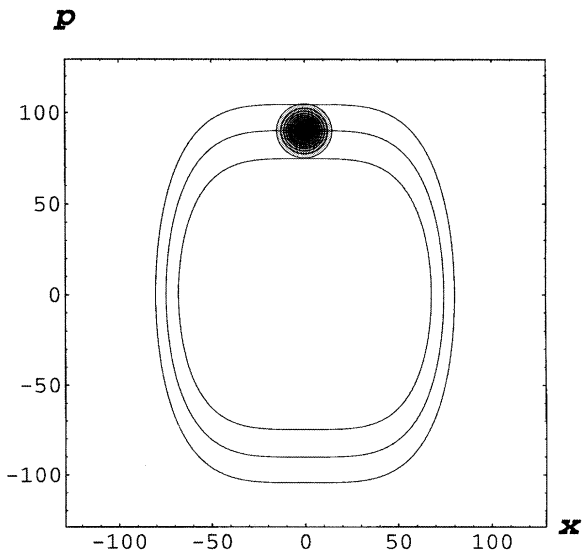

FIG. 1. Plot of contour lines of the Hamiltonian (2) for $\nu = 4$ (quartic oscillator) and the Husimi function (3) at $t = 0$. The curves $H = E(n)$ correspond to $N = 49$, 82, and 120, respectively.

 0031-9007/95/75(6)/990(4)$06.00

action

$$I[E] = \frac{1}{2\pi} \int_{H(p,x)<E} dp\, dx\,,$$
$$I(p,x) = I[H(p,x)]\,, \tag{4}$$

respectively. As time proceeds each part of the initial distribution seems to move along such a contour line with a velocity $|\,\mathrm{grad}\,H\,|$. Because of the form of the potential energy in (2), this speed is larger along the exterior contour lines than for the interior ones. As a consequence, the initially symmetrical distribution is not only shifted along the classical orbits but also stretched during this motion (see Fig. 2). Classically, this effect would continue forever and result in a distribution of increasingly finer spiral form. But it is well known [7] that classical and quantum evolutions deviate essentially from each other after a certain time t_{cl}, which depends on the initial state, the Hamiltonian, and the magnitude of $\hbar$ [8]. In the present case this moment is reached when the fast "head" of the packet and the slow "tail" meet in phase space and start to interact. The result of this interference in phase space (see Fig. 3) was described in Ref. [4] as "creation of small packets," and from the snapshots displayed there it was concluded that this nonclassical structure is "robust," i.e., persists for all times $t > t_{\mathrm{cl}}$.

This is not the case, since the initial state (1) lives essentially in a *finite-dimensional subspace* spanned by eigenfunctions of $\hat{H} = H(\hat{p},\hat{x})$ with eigenvalues $E(n_{\min}) \le E(n) \le E(n_{\max})$ (small components belonging to other energies may be neglected). Therefore only a finite number of frequencies occur in (3), whence the evolution is almost periodic and the initial coherent state

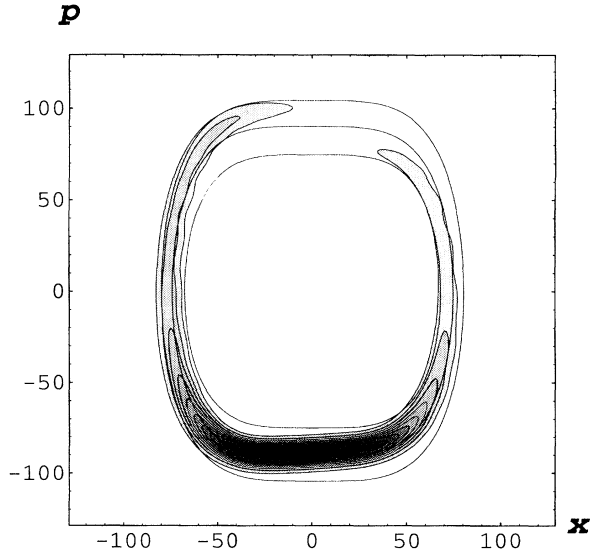

FIG. 2. Same as Fig. 1, but $t = 0.03\tau_0$; τ_0, see Eqs. (15) and (13).

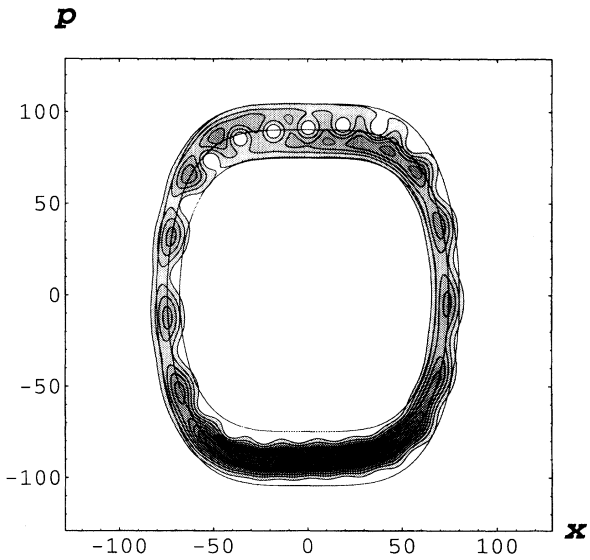

FIG. 3. Same as Fig. 1, but $t = 0.05\tau_0$.

is almost completely restored after some very long period T. More surprising, however, is the fact that at much earlier times the Husimi function (3) assumes again and again highly regular forms, where the original Gaussian seems to be split into a finite number of "Gaussians" of smaller amplitude (see Fig. 4). The maxima of such a string are distributed along the central classical orbit in such a way that the time needed to proceed from one maximum to the next one is always the same (T_0/M, if T_0 is the classical period of the central orbit and M is the number of peaks in the string). Each of these new peaks behaves like the initial one: In the beginning of the formation of the string the individual peaks become more narrow and increase in height, which corresponds to the inverse decay of the initial wave packet just before $t = 0$. After having reached a maximum of pronunciation the peaks decay, as did the initial peak immediately after $t = 0$. While it exists, the whole string rotates along the central classical orbit with local speed varying according to $|\,\mathrm{grad}\,H\,|$.

It should be noted that these orbits are not circles, as would be the case for the harmonic oscillator. Therefore the expectation values of p and x do not vanish for strings with *odd* M but oscillate with a period T_0/M (cf. Fig. 4). Because of the common growth and decay of all the peaks, the amplitudes of these oscillations are modulated by bell-shaped curves (Fig. 5). Similar conclusions can be drawn for $F_{p_0,x_0}(p_0,x_0,t)$, the square modulus of the autocorrelation function, by inspection of Figs. 1–4: In the beginning it oscillates with period T_0. When a chain of M peaks is present it oscillates with period T_0/M; note that here M can be *odd or even*. Because of contraction and spreading of the peaks, the amplitudes

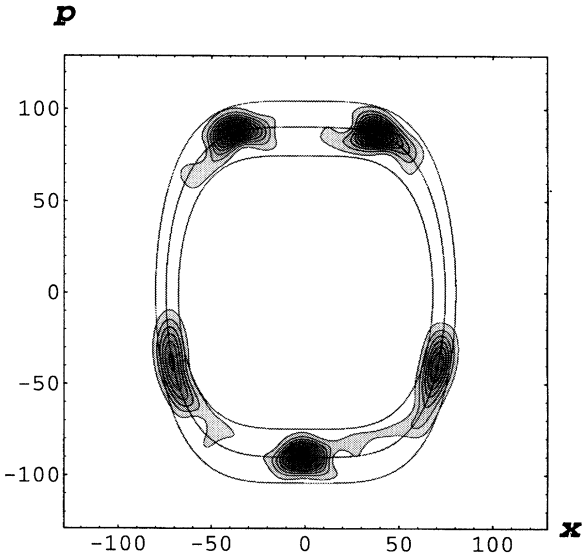

FIG. 4. Same as Fig. 1, but $t = 0.20\tau_0$.

of these oscillations are again modulated by bell-shaped curves.

All these effects are especially pronounced in the semiclassical regime where

$$n_{\min} \gg 1\,, \quad |n_{\max} - n_{\min}| \ll n_{\min}\,, \tag{5}$$

and hence $(n + n')/2 = \bar{n} \gg |\Delta n| = |n - n'|$ for all $n_{\min} \leq n, n' \leq n_{\max}$. Our explanation of the interference patterns rests on two properties of the Hamiltonian (2):

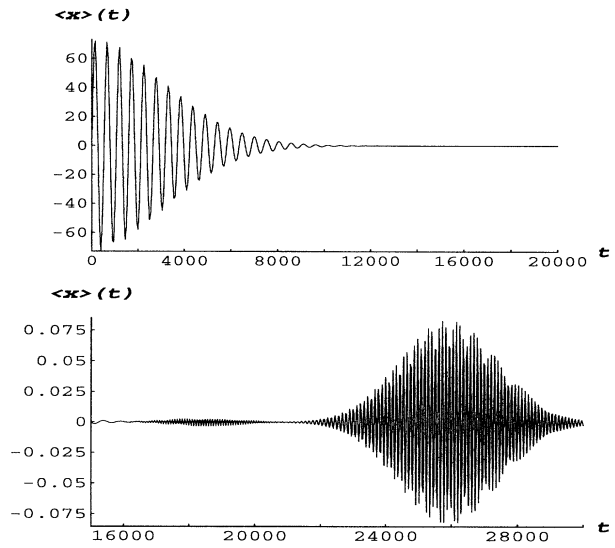

FIG. 5. Expectation value $\langle x \rangle$ as a function of time. Upper part: Oscillations reflecting the motion and spreading of the initial coherent state. Lower part: Oscillations caused by strings of seven and five peaks, respectively.

First, consider the functions

$$Q_{n,n'}(p,x) = \langle\, p,x \mid n\,\rangle\langle\, n' \mid p,x\,\rangle\,, \tag{6}$$

where $|\, n\,\rangle$ is the eigenfunction of $\hat{H}$ for the eigenvalue $E(n)$ and $|\, p,x\,\rangle$ is the coherent state centered at (p,x). In the semiclassical limit these functions assume the following form:

$$Q_{n,n'}(p,x) \approx C_{\bar{n},\Delta n}\, R_{\bar{n}}(I)\, e^{i\Delta n\Theta}\,, \tag{7a}$$

$$R_{\bar{n}}(I) = \exp\{-(\bar{\omega}^2/2\hbar\bar{E})(I - \bar{n}\hbar)^2\}\,. \tag{7b}$$

Here $\bar{E} = E(\bar{I})$, $\bar{\omega} = \omega(\bar{I})$, $E(I)$ is the inverse of the function $I[E]$, $\omega(I) = \partial E(I)/\partial I$, and $\bar{I} = \bar{n}\hbar$. $I = I(p,x)$ and $\Theta = \Theta(p,x)$ are the classical action and angle variables. Equations (7) emerge from numerical studies, analytical results for the limiting cases $\nu = 2$ (harmonic oscillator) and $\nu = \infty$ (square well), and from a semiclassical analysis [6]. Note that in (7) the Maslov index drops out in Δn and becomes negligible compared to $\bar{n}$.

The evolution of an operator $|\, n\,\rangle\langle\, n'\,|$ is given by the exponential $\exp[-it[E(n) - E(n')]/\hbar]$. Hence

$$F_{p_0,x_0}(p,x,t) = \sum_{n,n'} Q_{n',n}(p_0,x_0)\, Q_{n,n'}(p,x,t)\,, \tag{8}$$

$$Q_{n,n'}(p,x,t) = Q_{n,n'}(p,x)\, e^{-it[E(n)-E(n')]/\hbar}\,. \tag{9}$$

In numerical calculations this series may always be restricted to a finite sum ($n_{\min} \leq n, n' \leq n_{\max}$). In (8) a pair of terms with $n, n' = n_1, n_2$ and $n, n' = n_2, n_1$ represents a real phase-space function which is concentrated along the curve $I(p,x) = \hbar(n_1 + n_2)/2$ and has $n_1 - n_2$ nodes on this orbit. During a time interval t this function is shifted along the curve of constant action by the angle

$$\Theta_t = t[E(n_1) - E(n_2)]/\hbar(n_1 - n_2)\,, \tag{10}$$

as can be seen from (7) and (9).

The second property of the Hamiltonian which is needed for the explanation of the interference phenomena described before is related to the expansion of $E(I)$ around the mean energy.

$$E(I) = E_0 + \omega(I_0)\,\delta I + \tfrac{1}{2}\,\omega'(I_0)\,\delta I^2 + \cdots\,,$$
$$E_0 = E(I_0)\,, \quad I_0 = I(p_0,x_0)\,, \quad \delta I = I - I_0\,. \tag{11}$$

It can be shown [6] that for Hamiltonians of the form (2) and an energy range fixed by the initial coherent state the higher order terms in (11) may be neglected in the

semiclassical limit. In this case one obtains from (10) and (11)

$$\Theta_t \approx t\,[\,\alpha_0 + \beta_0(n_1 + n_2)\,], \tag{12}$$

$$\alpha_0 = \omega(I_0) - \omega'(I_0)\,I_0\,\hbar\,, \quad \beta_0 = \omega'(I_0)\,\hbar/2\,. \tag{13}$$

Equations (7), (9), and (12) show that all phase-space functions (9) occurring in the sum (8) which are concentrated on the same classical orbit move with the same angular velocity. It is therefore possible to combine all terms in (8) with $(n + n')/2 = \bar{n}$ (integer or half integer) into a single function of the form

$$\tilde{Q}_{\bar{n}}(p,x,t) \approx R_{\bar{n}}(I)\,\tilde{A}_{\bar{n}}(\Theta - t[\alpha_0 + 2\beta_0\bar{n}])\,. \tag{14}$$

This function has the form of a "profile" [function $\tilde{A}_{\bar{n}}$ with $\tilde{A}_{\bar{n}}(\Theta + \pi) = (-1)^{2\bar{n}}\tilde{A}_{\bar{n}}(\Theta)$] which sits on the orbit $I(p,x) = \bar{n}\hbar$ (function $R_{\bar{n}}$) and moves along this *Bohr orbit* ($\bar{n}$ integer) or *half-Bohr orbit* ($\bar{n}$ half integer) with constant angular velocity $\alpha_0 + 2\beta_0\bar{n}$. The term α_0 yields a shift in Θ which is the same for all relevant orbits ($n_{\min} \le \bar{n} \le n_{\max}$); the second term indicates that profiles sitting on adjacent orbits move with constant relative angular velocity. This is similar to classical mechanics, where the angular velocity $\omega(I)$ also varies with I; but combined with the discreteness of the admissible orbits this fact gives rise to the observed interference patterns. First, it is clear that at time $t = \tau_0$,

$$\tau_0 = 2\pi/\beta_0\,, \tag{15}$$

the second term becomes irrelevant, and the initial Gaussian is simply shifted along the central orbit. Next, consider the time $t = \tau_0/M$, M integer: Adjacent profiles are now shifted against each other by π/M so that only the profiles (14) with $\bar{n}$, $\bar{n} + M$, $\bar{n} + 2M$, ... add up in the same angle Θ and cancel each other at $\Theta + \pi$. Therefore a set of M peaks, equally distributed along the central trajectory, appears in the graphical representation of the Husimi function. Compared to the initial peak each of the new peaks is now reduced in height by a factor $1/M$, because the density normal to the orbits is thinned out by the relative motion of adjacent profiles. This relative motion also explains why the M peaks contract before the instant $t = \tau_0/2M$ and decay afterwards.

In a time series of plots of the Husimi function one will find strings consisting of M packets for all $M = 1,\ldots,M_{\max}$, where $M_{\max}$ is determined by the ratio of the length of the central orbit to the diameter of the initial distribution. Strings seen in the beginning of the evolution consist, in general, of almost identical peaks, whereas at later times the higher order terms neglected in (12) dissolve the regularity of the fine structure.

This research was supported by the Austrian Science Foundation (FWF) under Contract No. M0169-PHY.

Note added.—After submission of the paper we discovered that the interference effects considered here are known in quantum optics as "fractional revival of wave packets' [9,10]. The evolution of a localized wave function into a superposition of such functions, which corresponds to the splitting of a localized Husimi function into a chain of peaks, was explained in [11] on the basis of number theoretic considerations. Our approach which is based on Eq. (7) substantiates the heuristic arguments of [10] and shows that half-Bohr orbits have to be included in a satisfactory explanation of the phenomenon.

[1] H. Weyl, Z. Phys. **46**, 1 (1927); E. Wigner, Phys. Rev. **40**, 749 (1932).
[2] S. R. DeGroot and L. G. Suttorp, *Foundations of Electrodynamics* (North-Holland, Amsterdam, 1972); M. Hillary, R. F. O'Connell, M. O. Scully, and E. Wigner, Phys. Rep. **106**, 121 (1984).
[3] K. Husimi, Proc. Phys. Math. Soc. Jpn. **22**, 264 (1940).
[4] K. Takahashi, Prog. Theor. Phys. Suppl. **98**, 109 (1989).
[5] For a deeper discussion of the relation between classical and quantum phase-space distributions, see, e.g., E. Prugovečki, *Stochastic Quantum Mechanics and Quantum Spacetime* (Reidel, Dordrecht, 1986).
[6] P. Kasperkovitz and M. Peev (to be published).
[7] S. L. Robinson, J. Math. Phys. **34**, 2185 (1993).
[8] Note that in our definition of $t_{\rm cl}$ the classical distribution function is compared to the Husimi function. Comparison with the Wigner function yields disagreement at earlier times, whereas classical and quantum expectation values of smooth observables such as x or p begin to diverge at later times (cf. Fig. 5).
[9] J. H. Eberly, N. B. Narozhny, and J. Sanchez-Mondragon, Phys. Rev. Lett. **44**, 1323 (1980).
[10] M. Nauenberg, C. Stroud, and J. Yeazell, Sci. Am. **270**, No. 6, 24 (1994), and references therein.
[11] I. Sh. Averbukh and N. F. Perelman, Phys. Lett. A **139**, 449 (1989).